ORIGINAL PAPER

Optimization in Solvent Selection for Chlorin e6 in Photodynamic Therapy

Shubhajit Paul · Paul Wan Sia Heng · Lai Wah Chan

Abstract The photophysical properties of chlorin e6 (Ce6) in twelve different protic, aprotic and non-polar solvents were investigated using ultraviolet–visible and fluorescence spectroscopic methods. Solvatochromic effects were determined by the changes in quantum yield, Stokes shift, fluorescence half-life and excited state dipole moments of Ce6 in the different solvents. The absorption shifts observed in different solvents were further analyzed using the Kamlet-Abboud-Taft model and the nature of solute-solvent interactions between Ce6 and different protic and aprotic solvents was elucidated. The quantum yields were found highest in protic solvents (except water), followed by aprotic and non-polar solvents. Solvent polarity parameters showed a linear increasing trend with Stokes shift and fluorescence half-life, which indicated the presence of Ce6-solvent interaction. Using the Kamlet-Abboud-Taft model, a direct correlation between the solvent polarity parameters and absorption shift was observed, which substantiated the existence of Ce6-solvent interaction by hydrogen bond formation. The excited state dipole moments in specific protic and aprotic solvents were found to be higher than the ground state dipole moments, implying a more polar nature of Ce6 during excited state transition.

Keywords Chlorin e6 · Stokes shift · Quantum yield · Kamlet-Abboud-Taft model

S. Paul · P. W. S. Heng · L. W. Chan (✉)
Department of Pharmacy, Faculty of Science,
National University of Singapore,
18 Science Drive 4,
Singapore 117543, Singapore
e-mail: phaclw@nus.edu.sg

Introduction

The solute-solvent interaction is an important consideration for organic dyes as solvents often facilitate changes in the electronic state distribution of dye molecules upon excitation [1]. One of the simplest techniques to study such interactions is with the use of ultraviolet–visible (UV–vis) absorption spectra and fluorescence spectra. Interactions of a solute (dye) with various solvents usually correlate with shifts in absorption wavelengths. This shift is commonly termed as solvatochromism and depends on the electronic structures of the dye and the solvent molecules [2]. Solvatochromism is mainly caused by the differential solvation of the ground and the first excited state of the solute molecule of interest. The positive or negative shift in the λ_{max} depends on the relative stabilization of the ground and excited states. The solvent-induced shift in electronic spectra has been widely used to study the changes in electronic distribution in excited state of solute molecules [3]. Fluorescent probes have been extensively used for determination of solvent polarity in the studies of heterogeneous media as well as biochemical and biological systems [4, 5]. An understanding of the excited state properties not only helps in the classification of a new molecule but also determines the potential performance of compounds after photoexcitation. For example, fluorescent active drugs have been widely used in the treatment of superficial cancers by photodynamic therapy. The underlying mechanism lies in the photoexcitation of the fluorescent active drug molecules, which after excitation are promoted to triplet state and generate singlet oxygen [6]. These generated species are highly reactive free radicals, which are capable of destroying the localised tumor cells. The efficiency of singlet oxygen generation depends on spontaneous $\pi-\pi^*$ transition from ground to triplet state. In other words, these events are affected by solute-solvent

interaction and microenvironment of the solute. Some of the potential factors which may affect the photophysical properties of therapeutic dyes include aggregation and solvent-induced monomerization of the dye molecules. Aggregation of dyes is particularly notable in aqueous solutions by H-bonding between dye molecules, although some aggregates could also result from strong hydrophobic bonds in certain solvents [7]. Some solvents form H-bonding with the dye molecules, thus breaking down the aggregates. Therefore, understanding of certain photophysical parameters like quantum yield, fluorescence half-life and excited state dipole moment can help to illustrate the photophysical nature of the fluorophore in excited state [8]. The dipole moments of a molecule depend on its electronic distribution, which is affected by the polarity, dielectric constant and polarizability of the surrounding medium. Therefore, the resultant dipole moment determines polarity of the fluorophore [9]. In addition, variation in fluorescence half -life in different solvents can delineate the underlying solute-solvent interactions. A lower fluorescence half- life value indicates nonspontaneous transformation from ground to excited state, which could probably be indicative of the aggregated state of the dye molecules [10].

Several solvent studies were conducted on the metallo-porphyrin, porphyrin complexes and highly substituted porphyrin compounds [11–13]. However, studies on the porphyrin macrocyle and its photophysical changes in the presence of different solvents are still limited. Chlorin e6 (Ce6) is an example of a photoactive dye with simple porphyrin nucleus and it is used in photodynamic therapy to treat mucosal tumors (Fig. 1a) [14]. Its therapeutic efficacy is often limited by the formation of aggregates, which drastically reduces the quantum yield of Ce6 and thus, the efficiency for photodynamic treatment. Hence, the aim of this study was to investigate the appropriateness of various solvents for Ce6 in order to produce high fluorescence activity for photodynamic therapy through specific favorable solute-solvent interactions. Therefore, the influence of various solvents on the photophysical properties of Ce6 in ground and excited states was investigated. The quantum yield, fluorescence half life and excited state dipole moments of Ce6 in different solvents were evaluated to provide a better understanding of the excited state properties of Ce6 and conditions correlated to aggregate formation,

Theoretical Background

The commonly used equations in fluorescence spectroscopy are proposed by Lippert and Mataga et al. [15]. These equations are based on the Onsager reaction field theory, which assumes that the fluorophore is a point dipole residing in the centre of a spherical cavity with radius, a, in a homogeneous and isotropic dielectric medium with relative permittivity, ε. However, the Lippert-Mataga equation does not hold true for non-specific interaction, specific fluorophore-solvent interaction such as hydrogen bonding or electron pair acceptor-donor interaction. Furthermore, Lippert equation was also reported to be inaccurate for estimating the radius of molecules with an ellipsoidal shape [8]. Kawski and co-workers developed a simple quantum mechanical second-order perturbation theory of absorption and fluorescence band shifts in different solvents of varying permittivity and refractive index. According to this theory, the following equations were proposed [16]:

$$v_a - v_f = m_1 f(\varepsilon, n) + constant \tag{1}$$

$$v_a + v_f = -m_2[f(\varepsilon, n) + 2g(n)] + constant \tag{2}$$

where v_a and v_f are the energy of absorption and emission respectively and their difference is denoted by Stokes shift. n is the refractive index of the solvent medium, $f(\varepsilon,n)$ and $g(n)$ are the polarity parameters and their experimental estimate is given by

$$f(\varepsilon, n) = \frac{2n^2 + 1}{n^2 + 2}\left[\frac{\varepsilon - 1}{\varepsilon + 2} - \frac{n^2 - 1}{n^2 + 2}\right] \tag{3}$$

and

$$g(n) = \frac{3(n^4 - 1)}{2(n^2 + 2)^2} \tag{4}$$

while

$$m_1 = \frac{1\left(\mu_e - \mu_g\right)^2}{hca^3} \tag{5}$$

and

$$m_2 = \frac{2\left(\mu_e^2 - \mu_g^2\right)}{hca^3} \tag{6}$$

where h is the Planck's constant, c is the velocity of light in vacuum and a is the radius of the solute. The parameters, m_1 and m_2, are the slopes of the linear plots described by Eqs. (1) and (2) respectively. The dipole moments at ground (μ_g) and excited states (μ_e) can be given as

$$\mu_g = \frac{m_2 - m_1}{2}\left[\frac{hca^3}{2m_1}\right]^{\frac{1}{2}} \tag{7}$$

and

$$\mu_e = \frac{m_2 + m_1}{2}\left[\frac{hca^3}{2m_1}\right]^{\frac{1}{2}} \tag{8}$$

or

$$\mu_e = \frac{m_2 + m_1}{m_2 - m_1}\mu_g, m_2 > m_1 \qquad (9)$$

According to Ravi et al., the excited state dipole moment is calculated by [18]:

$$v_a - v_f = 11307.6\left[\left(\frac{\Delta\mu}{\Delta\mu_B}\right)^2\left(\frac{a_B}{a}\right)^3\right]E_T^N + constant \qquad (10)$$

where $\Delta\mu_B$ is the dipole moment change on excitation and a_B is the onsager radius for betaine dye. The values of $\Delta\mu_B$ and a_B are 9 D (debye) and 6.2 Å respectively. E_T^N is the normalized transition energy which can be calculated for each solvent using water and tetramethylsilane (TMS) as extreme reference solvents with the following equation:

$$E_T^N = \frac{E_T(solvent) - E_T(TMS)}{E_T(water) - E_T(TMS)}$$
$$= \frac{E_T(solvent) - 30.7}{32.4} \qquad (11)$$

Therefore, the change in the dipole moment is determined by

$$\Delta\mu = \mu_e - \mu_g = \left[\frac{m \times 81}{(6.2/a)^3 \times 11307.6}\right]^{\frac{1}{2}} \qquad (12)$$

where m is the slope of the linear plot of E_T^N versus Stokes shift $(v_a - v_f)$ described by Eq. (10).

Materials and Methods

Materials

Chlorin e6 was purchased from SPE Chemical Co. Ltd. (Shanghai, China) and used as supplied. All the solvents used in this study were from Merck (Singapore) and of spectroscopic grade. The solvents were of three primary classes, polar protic (water, methanol, ethanol, isopropanol and glycerol), polar aprotic (acetone, acetonitrile, dimethylsulfoxide [DMSO] and tetrahydrofuran [THF]) and non-polar (dichloromethane [DCM], dioxane and hexane) solvents. Rhodamine 6 G (Sigma Aldrich, Singapore) was used as standard for quantum yield calculation.

Method

Absorption spectra and fluorescence emission spectra were recorded in a UV–vis spectrophotometer (Shimadzu 2101PC, Japan) and spectrofluorometer (Fluoromax-P Jovin Yvon, USA) respectively. For all the fluorescence measurements, excitation wavelength and slit width were set at 405 nm and 2 nm, respectively. Fluorescence lifetime measurements were performed with a time-correlated single-photon counting fluorometer (Fluoromax-4 Jovin Yvon, USA) for all the solvents. Ce6 ground state geometry was optimized by employing semi-empirical AM1 parameterization using a molecular modelling software (Hyperchem 8.0, Hypercube Inc., USA). The value of solute cavity radius (a_0) was calculated from the molecular volume of Ce6 according to the following equation [19]:

$$a_0 = (3M/4\pi\delta N)^{1/3} \qquad (13)$$

where δ is the density of the solute molecule, M is the molecular weight of the solute and N is the Avogadro's number.

Fluorescence quantum yield (ϕ) which represents the activity of a fluorophore, is defined as the ratio of number of photons emitted to number of photons absorbed. Therefore, quantum yield values theoretically lie within 0 to 1. Quantum yields of Ce6 in each of the solvents were calculated using the following equation,

$$\frac{\phi_1}{\phi_2} = \frac{(1 - 10^{A_2})}{(1 - 10^{A_1})}\frac{n_1^2}{n_2^2}\frac{\alpha_1}{\alpha_2} \qquad (14)$$

where A is the absorbance, n is the refractive index and α is the area under the fluorescence emission spectra for

Fig. 1 **a** Molecular structure of Ce6 and **b** isosurfaces of HOMO and LUMO orbitals of Ce6 for first singlet excited state

a

b

HOMO   LUMO
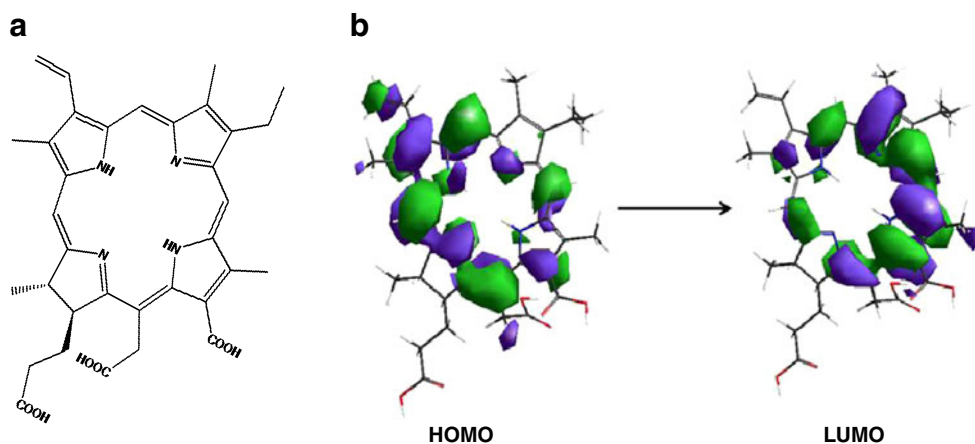
standard (sample 1) and test (sample 2) respectively. Quantum yield was determined using rhodamine 6 G as standard (ϕ=0.64 in ethanol). All the measurements were carried out at room temperature (298 K), keeping the dye concentration very low in order to avoid self-absorption. For quantum yield determination, Ce6 concentration in each of the solvents was adjusted such that absorbance value was around 0.2 to ensure that roughly equal number of photons was absorbed. Fluorescence emission spectra were then collected subsequently for each of the solvents.

Results and discussion

Photophysical Properties of Ce6 in Different Solvents

Ce6 belongs to the porphyrin class of photosensitizers that produces intense fluorescence emission in the red region. Due to electron transfer through the porphyrinic macro-cycle, charge transfer bands, characterized by large Stokes shift values (generally>200 nm) are observed for chlorin-based photosensitizers [17]. Figure 1b shows the isosurfaces of HOMO and LUMO orbitals of Ce6 in the first singlet excited state. Theoretical calculations obtained from Hyper-chem semi-empirical model showed the first singlet excited state of Ce6 at 376 nm (in gas phase). This corresponded to experimentally observed Soret band around 400 nm and clearly revealed that electron transfer from HOMO to LUMO orbital was largely confined to pyrrole nucleus of porphyrin macrocycle due to the presence of highly polarisable NH groups.

The UV–vis spectra of Ce6 in three distinct classes of solvents are shown Fig. 2. The wavelength of maximum absorption and its corresponding emission for each of the solvents are shown in Table 1. The polar protic solvents exhibited Soret band at around 403 nm and Q band at 664 nm with notable deviations shown by water and glyc-erol (Fig. 2a). As can be seen, sharp Soret and Q bands were observed for all the protic solvents except water. A broad spectrum along with spectral shifts of Soret and Q bands suggested extensive intermolecular aggregation of Ce6 in water. For polar aprotic solvents, clear Soret band around 403 nm (except DMSO, λ_{max}=407 nm) and Q band at 664 nm were found (Fig. 2b). Figure 2c shows the UV–vis spectra of Ce6 in non-polar solvents. Soret and Q bands in this class were found from 401 nm to 405 nm and 667 nm respectively. Increased baseline values of Ce6 in specific solvents, such as water, DMSO and hexane suggested its strong hydrophobicity in those solvents. Figure 3 collective-ly shows the fluorescence emission spectra of Ce6 in differ-ent class of solvents. A couple of important observations were noted here. For all the solvents, emission occurred at
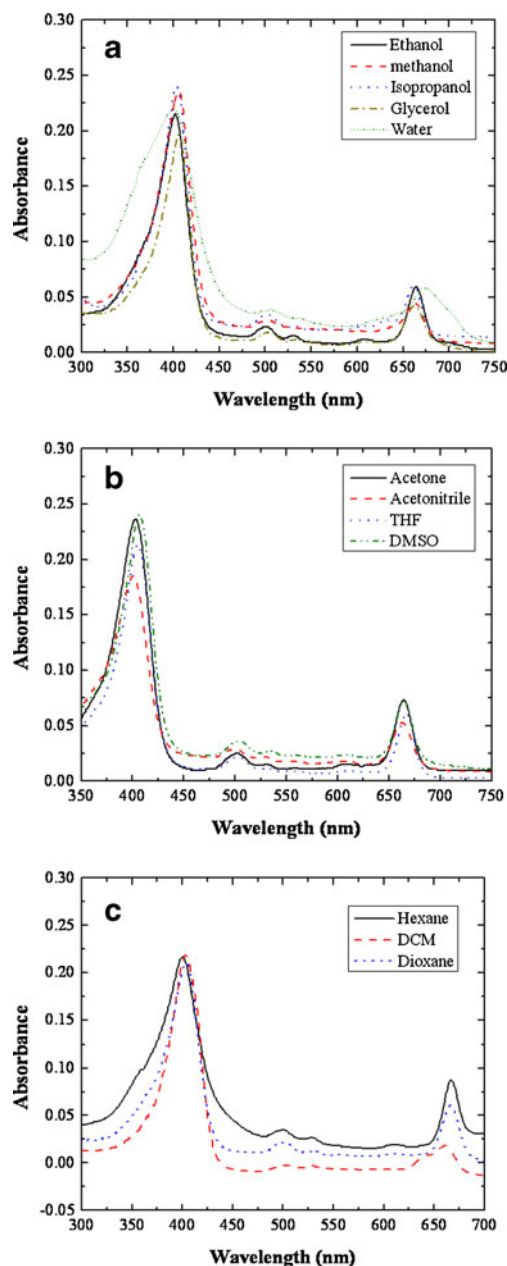

Fig. 2 UV–VIS absorption spectra of Ce6 in **a** polar protic, **b** polar aprotic and **c** non-polar solvents

higher wavelengths (positive Stokes shift) than the absorp-tion, implying a π-π^* transition in the excited state. The λ_{em} varied from 651 nm for water to 669 nm for other polar and apolar solvents. Although absorbance values of all the sol-vents were kept relatively constant, the fluorescence emis-sion intensities of the solvents varied significantly. From the polar protic class, the lowest emission intensity was ob-served for water, followed by glycerol while alcohols showed highest fluorescence intensity. The polar aprotic class of solvents generally showed higher fluorescence in-tensity with the exception of DMSO, which was found close to water. The non-polar solvent like DCM and dioxane

Table 1 Absorption and emission maxima of Ce6 in various solvents and corresponding polarity parameters

Solvent	λ (nm)		ε	n	$f(\varepsilon,n)$	$g(n)$	Ce6 absorption (υ_a) and emission (υ_f) energy			
	Abs	Em					υ_a	υ_f	$\upsilon_a - \upsilon_f$	$\upsilon_a + \upsilon_f$
Water	401	652	80.7	1.33	0.914	0.082	24938	15337	9601	40275
Methanol	405	666	32.7	1.33	0.855	0.081	24691	15015	9676	39706
Ethanol	402	667	24.5	1.36	0.813	0.086	24876	14993	9883	39869
Isopropanol	404	664	20.3	1.38	0.779	0.09	24752	15060	9692	39812
Glycerol	407	667	42.5	1.47	0.835	0.1	24570	14993	9577	39563
Acetonitrile	400	666	38.8	1.34	0.866	0.083	25000	15015	9985	40015
Dimethylsulfoxide	407	667	47.2	1.48	0.841	0.102	24570	14993	9577	39563
Acetone	403	667	20.7	1.36	0.790	0.086	24814	14994	9820	39808
Tetrahydrofuran	405	669	7.52	1.41	0.547	0.093	24691	14948	9743	39639
1,4 dioxane	404	669	2.20	1.42	0.04	0.095	24752	14948	9804	39700
n-hexane	401	667	1.88	1.37	−0.002	0.089	24938	14993	9945	39931
Dichloromethane	405	670	2.20	1.46	0.014	0.099	24570	14925	9645	39495

showed higher fluorescence than that of hexane, which was also similarly close to water. The strikingly higher intensity for dioxane could be explained on the basis of possible H-bond formation with the pyrrolic NH groups of Ce6, which increased polarity of the medium [18]. Marked reduction of fluorescence intensity of the afore-mentioned solvents could be ascribed to non-spontaneous transition to the excited state because of strong hydrophobicity or aggregation in those solvent environments. The areas under the fluorescence emission spectra were calculated using Origin Pro 8.1 software (Origin Lab Inc., USA) to determine the quantum yield (ϕ_F) of Ce6 in each of the solvents (Table 2). From Eq. (14), quantum yield is directly dependent on the fluorescence intensity and ϕ_F varied largely for different solvents. ϕ_F was found highest in alcohols and lowest in water. Among the non-polar solvents, dioxane showed higher ϕ_F value, while aprotic solvents exhibited moderate ϕ_F values less than that of alcohols. Interestingly, a significantly lower ϕ_F was observed for polar solvents like glycerol and DMSO. ϕ_F has been reported to be higher in glycerol for various dyes. This was attributed to the high viscosity of glycerol, which restricted the rotational movements of the fluorophore and thus the excited state energy was released mostly through the relaxation pathways, resulting in high ϕ_F [19]. From the initial observations, it was postulated that deviations of ϕ_F, as well as spectral features, were likely to be due to specific solute-solvent interactions such as H-bonding between fluorophore and solvent and aggregation of Ce6 through intermolecular H-bonding. The influence of the various polarity parameters on Ce6 photophysical properties was further investigated. Figure 4 shows a linear dependence of Soret band energy (υ_a) with Reichardt polarity parameter [$f(n^2)$]. It has been reported that extensive H-bonding with solvent molecules results in non-planarity of

porphyrin macrocycle [20]. Since Soret band energy (cm^{-1}) is inversely related with λ_{max}, from Fig. 4 it could be deduced that an increase in solvent polarity resulted in further red shift of Ce6 in these solvents. A fairly good correlation (r^2=0.88) was obtained between Soret band energy and Reichard polarity parameter, excluding methanol and hexane. This indicated that the extent of non-planarity of porphyrin macrocycle is dependent on solvent polarity, however profound H-bonding in methanol had caused further non-planarity in Ce6 molecule and thus deviated from the plot. Significant deviations for non-polar solvent like hexane suggested weak bond-dipole interactions were the major attractive solvation forces between solute and solvent resulting in least non-planarity of the Ce6 nucleus in hexane. This suggested that specific H-bonding existed between Ce6 and polar group of solvents. To corroborate the evidence, dependence between Lipert's polarity parameter [$f(\varepsilon,n)$] and Stokes shift was investigated. Figure 5a shows no dependence between $f(\varepsilon,n)$ and Stokes shift, clearly suggesting specific solute-solvent interaction [8]. Therefore, Chamma-Viallet modified polarity parameter [$f(\varepsilon,n)+2g(n)$] of different solvents were plotted against ($\upsilon_a+\upsilon_f$) and the results showed the presence of two distinct clusters in the plot (Fig. 5b). The invariant cluster (circled) mainly comprised polar solvents except glycerol and DMSO suggesting the presence of H-bonding between Ce6 and polar group of solvents. Interestingly, these two solvents along with non-polar solvents showed a fairly good correlation with a negative slope (r^2=0.81). The significant deviation of glycerol and DMSO from the cluster suggested less favorable orientation for H-bonding. Next, the Soret band energy values were plotted against polarizability of different solvents. Polarizability (π^*) measures the ability of the solvent to stabilize a charge or a dipole by virtue of its dielectric effect. The π^* scale runs from 0.0 for cyclohexane to 1.0 for DMSO. Figure 6a shows
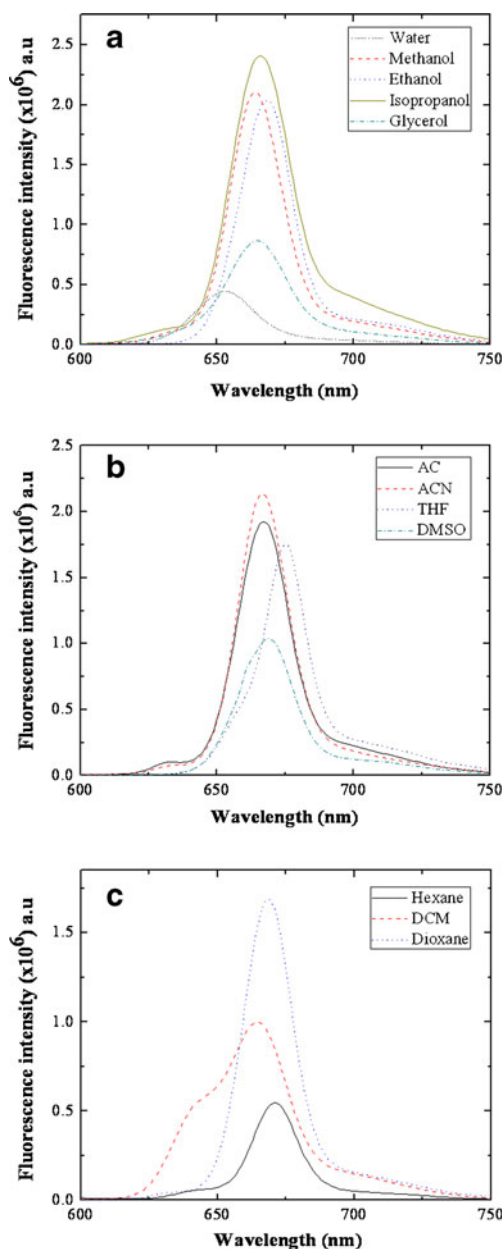
Fig. 3 Fluorescence emission spectra of Ce6 in **a** polar protic, **b** polar aprotic and **c** non-polar solvents

the variations of Soret band energy with solvent polarizability, with glycerol and DMSO deviating from the linear relationship. An increase in λ_{max} with π^* indicated increased capability of the solvent to form H bonds in solution [17]. Significant deviation shown by glycerol and DMSO further suggested that H-bonding in these solvents was somehow restricted. The unusual behaviour of these solvents could be explained on the basis of intermolecular dye aggregation. Dye aggregation is a commonly observed phenomenon, where strong hydrophobicity in the solvent medium results in intermolecular association of dye molecules. Such association reduces the availability of free dye molecules to interact with

neighbouring solvent molecules. In the present study, extent of Ce6 aggregation reduced the availability of free Ce6 molecules for H-bonding with the afore-mentioned solvents. Furthermore, the viscosity of DMSO and glycerol (1.99 and 1400 cp respectively) was relatively higher than that of other solvents, which might have affected the flexibility of Ce6 molecules and rendered them in a state of orientation, which was susceptible to aggregate formation [21]. This was evidenced by slightly higher anisotropy values of Ce6 in DMSO and glycerol (~ 0.08), compared to other solvents (< 0.005), suggesting rotational movement of Ce6 was substantially restricted in the presence of these solvents.

The postulation of aggregate formation in the afore-mentioned solvents provides an answer for the low ϕ_F values in glycerol and DMSO. In order to further substantiate the postulation, the influence of fluorescence half-life (τ_F) on protic and aprotic solvents was investigated. As a rule, the dependence between τ_F and ET_{30} suggests specific solute-solvent interactions such as H-bonding [10]. ET_{30} value of a solvent is defined as the amount of energy (with respect to water) required to promote one mole of the standard fluorophore, dissolved in that specific solvent, from its electronic ground state to its first excited state. A high ET_{30} value of the solvent is therefore associated with higher polarity and greater stabilization effect on the fluorophore [8]. Figure 6b shows the variation of τ_F with solvent polarity parameter ET_{30}. As can be seen, significant deviations from linear dependence were observed for water, glycerol and DMSO. This could be ascribed to factors such as aggregation of Ce6. Table 2 represents the fluorescence half-life of Ce6 in different solvents. Interestingly, water showed the lowest τ_F, followed by non-polar solvents. Polar solvents showed a significant increase in τ_F with the exception of glycerol and DMSO, whose τ_F values were found to be intermediate. A low half-life value indicates a non-spontaneous transition from ground to excited state, thus suggesting the possible existence of fluorophore aggregates in the medium [22]. Hence, the typical behaviours of specific polar solvents such as, water, glycerol and DMSO appeared to preferentially favor aggregate formation with concomitant low τ_F and ϕ_F values. In case of non-polar solvents, weak van der Waals force of interaction existed possibly because of Ce6 aggregation, which was accounted for the low ϕ_F and τ_F values of Ce6 in these solvents.
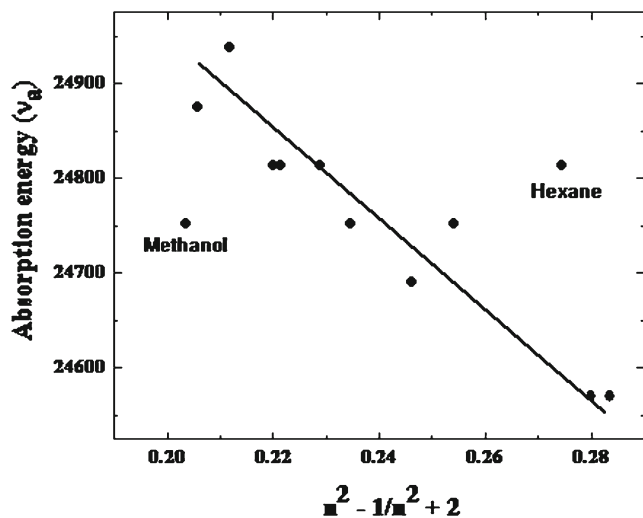
Determination of Excited State Dipole Moment

In the next stage, determination of the dipole moment of Ce6 in protic and aprotic classes of solvents was carried out. Determination of excited state dipole moment is an important consideration as it would reveal the excited state properties such as polarity, geometrical structure and course of photochemical transformations [23]. The conventional

Table 2 Solvent parameters, fluorescence half-life and quantum yield of Ce6 in various solvents

Solvent	E_T^N	π^*	α	β	τ_F (ns)	Φ_F
Water	1	1.09	1.17	0.18	1.13	0.18
Methanol	0.762	0.63	0.92	0.62	2.27	0.75
Ethanol	0.654	0.54	0.83	0.77	2.76	0.77
Isopropanol	0.546	0.48	0.76	0.95	2.97	0.83
Glycerol	0.812	0.73	0.98	0.52	1.59	0,39
Acetonitrile	0.46	0.75	0.19	0.31	2.21	0.64
Dimethylsulfoxide	0.386	1	0	0.76	1.7	0.35
Acetone	0.355	0.71	0.08	0.48	2.21	0.63
Tetrahydrofuran	0.207	0.58	0	0.55	2.4	0.60
1,4 dioxane	0.164	0.55	0	0.37	1.13	0.38
n-hexane	0.009	−0.08	0	0	1.09	0.14
Dichloromethane	0.052	0.28	0	0	1.07	0.29

equations for determination of excited state dipole moment are those described by Lippert-Mataga, Chamma-Viallet and Bakhshiev et al. [15]. However, in the case of specific solute-solvent interaction, non-linearity of the plots does not allow accurate determination of excited state dipole moment. In such cases, Eq. (10) as described by Ravi et al. is used. Semi-empirical molecular modelling AM1 was carried out using Hyperchem software for structural geometry optimization to calculate the ground state dipole moment. The molecular volume obtained was used in Eq. (13) to calculate the solute cavity radius of Ce6. The solute cavity radius and ground state dipole moment were found to be 5.14 Å and 5.7 D respectively. Figure 6c shows variation of Stokes shift with normalized transmission energy E_T^N. Water, glycerol and DMSO showed marked deviation and were not considered in the following correlation analysis. Stokes shift for alcoholic solvents and selected aprotic solvents showed a good correlation with E_T^N ($r^2 > 0.9$) and the excited state dipole moment was calculated from the slope

Fig. 4 Plot of Soret band energy vs. Reichard polarity parameter

of the graph as given in Eq. (10). The excited state dipole moments of Ce6 in these solvents were found to be higher than that of the ground state of Ce6 alone (Table 3). These findings suggested the occurrence of enhanced π-π^* transition of Ce6 in these solvents, which existed with higher polarity in the excited state.

Kamlet-Abboud-Taft (KAT) Model

The effect of solvents on absorption energy had been demonstrated by the Kamlet-Abboud-Taft (KAT) model [24]. The model proposed by Kamlet et al. is composed of solvatochromic parameters π^*, α and β, a linear combination of which is correlated with absorption energy of a fluorophore in different solvents. KAT model is shown by Eq. (15):

$$\nu_a = \nu_0 + s\pi^* + a\alpha + b\beta \tag{15}$$

KAT model provides the advantage of incorporating all the relevant polarity parameters in a linear form to illustrate specific solute-solvent interactions. Values of π^* for various non-chlorinated, non-protonic aliphatic solvents with a single dominant bond dipole, have been shown to be generally proportional to molecular dipole moment. The α scale of polar protic (H-bond donor) solvents describes the ability of the solvent to donate a proton in a solvent-to-solute hydrogen bond. The β scale of polar aprotic (H-bond acceptor) solvents provides a measure of the solvent's ability to accept a proton (donate an electron pair) in a solute-to-solvent H-bond. These parameters of different solvents used in this study are shown in Table 2. The coefficients of KAT parameters were obtained by fitting the absorption energy of different solvents in this model by multiple linear regression and shown in Table 3. When absorption energies of all the solvents were fitted in the model, a poor correlation was found ($r^2 = 0.52$). This showed that protic and aprotic solvents had specific interactions with Ce6 on the basis of their

Fig. 5 Plot of **a** Stokes shift vs. Lipert's polarity parameter and **b** ($\upsilon_a + \upsilon_f$) vs. Bakshievs polarity parameter
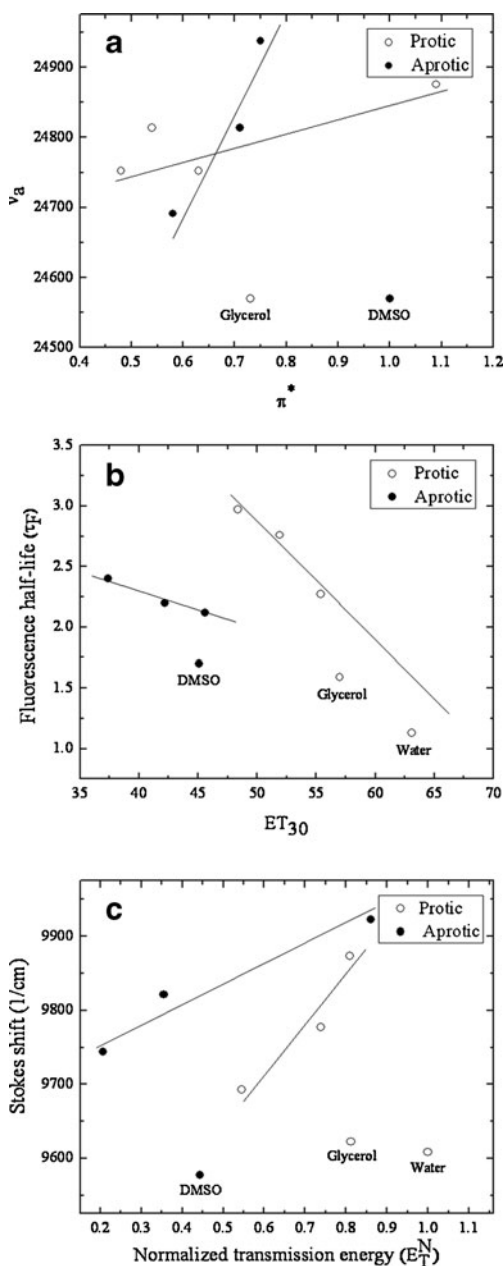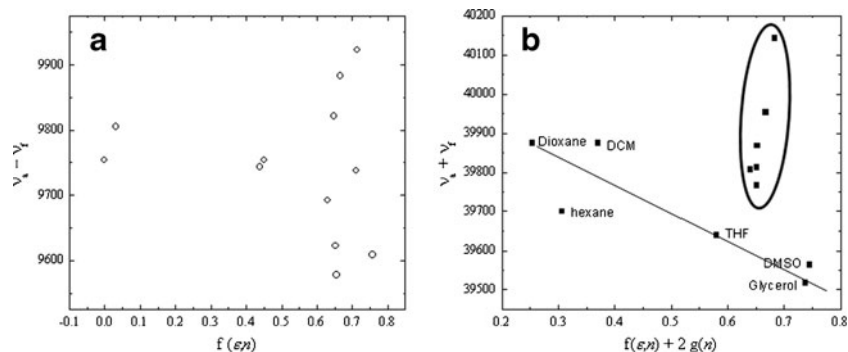

H-bond acceptor and donor capabilities. Interestingly, protic solvents except water showed excellent correlation (> 99 %). When water was included, correlation coefficient was lowered to 0.77. The decrease in linearity could be ascribed to extensive aggregate formation, which affected the solute-solvent interaction. Similar results were obtained for polar aprotic solvents, which also showed more than 99 % correlation between absorption energy and KAT parameters. This elucidated the specific solute-solvent interaction, i.e., H-bonding abilities of protic and aprotic solvents with Ce6. Excellent linearity with correlation above 0.99 indicates successful applicability of KAT equation to model solvent effect on porphyrin-based photosensitizer like Ce6. Moreover, excellent fitting of glycerol and DMSO in contrast to water further suggests that the extent of aggregate formation in these solvents were lower than in water.

Conclusion

Specific solute-solvent interaction was observed for Ce6 with protic and aprotic solvents. These solvents exhibited H-bonding with Ce6, while intermolecular Ce6 aggregation was observed particularly in water, glycerol, DMSO and other non-polar solvents. Aggregation and H-bonding were elucidated using fluorescence quantum yield, half-life and KAT model parameters for the various solvents. Specific solvents such as alcohols, acetone, acetonitrile and THF facilitated high fluorescence quantum yield, half-life and excited state dipole

Fig. 6 Plots of **a** Soret band energy vs. polarizability, **b** fluorescence half-life vs. transition energy and **c** Stokes shift vs. normalized transition energy of Ce6 in polar protic and aprotic solvents

Table 3 KAT model parameters and excited state dipole moments of selected protic and aprotic solvents

Kamlet-Taft correlation					Excited state Dipole moment (D)
Solvent type	s	a	b	Correlation coefficient	
Protic	−2508	−3960	−3060	0.997	7.49
Aprotic	−9981	34714	19385	0.992	6.71

moment. All these properties indicated that Ce6 was in aggregate-free state and more polar after excited state transition in those solvents. The information about the photophysical properties of these solvents will be useful while selecting a suitable vehicle for preparing pharmaceutical dosage forms of Ce6.

References

1. Rauf MA, Graham JP, Bukallah SB, Al-Saedi MA (2009) Solvatochromic behavior on the absorption and fluorescence spectra of Rose Bengal dye in various solvents. Spectrochim Acta A Mol Biomol Spectrosc 72:133–137
2. Umadevi M, Suvitha A, Latha K, Rajkumar BJ, Ramakrishnan V (2007) Spectral investigations of preferential solvation and solute-solvent interactions of 1,4-dimethylamino anthraquinone in CH_2Cl_2/C_2H_5OH mixtures. Spectrochim Acta A Mol Biomol Spectrosc 67:910–915
3. McRae EG (1957) Theory of solvent effects on molecular electronic spectra. Frequency shifts. J Phys Chem 61:562–572
4. Beddard GS, West MA (1981) Fluorescent probes. Academic, London
5. Wehry L (1990) Effects of molecular environment on fluorescence and phosphorescence. In: Guilbault GG (ed) Practical fluorescence, 2nd edn. Dekker, New York
6. Jang B, Choi Y (2012) Photosensitizer-conjugated gold nanorods for enzyme-activatable fluorescence imaging and photodynamic therapy. Theranostics 2:190–197
7. Biswas S, Ahn HY, Bondar MV, Belfield KD (2012) Two-photon absorption enhancement of polymer-templated porphyrin-based J-aggregates. Langmuir 28:1515–1522
8. Reichardt C (2004) Solvents and solvent effect in organic chemistry, 3rd edn. WILEY-VCH Verlag GmbH & Co., Weinheim
9. Mannekutla JR, Mulimani BG, Inamdar SR (2007) Solvent effect on absorption and fluorescence spectra of coumarin laser dyes: evaluation of ground and excited state dipole moments. Spectrochim Acta A Mol Biomol Spectrosc 69:419–426
10. Gómez ML, Previtali CM, Montejano HA (2003) Photophysical properties of safranine O in protic solvents. Spectrochim Acta A Mol Biomol Spectrosc 60:2433–2439
11. Guo H, Jiang J, Shi Y, Wang Y, Dong S (2007) Solvent effects on spectrophotometric titrations and vibrational spectroscopy of 5,10,15-triphenyl-20-(4-hydroxyphenyl)porphyrin in aqueous DMF. Spectrochim Acta A Mol Biomol Spectrosc 67:166–171
12. Wang X, Lu M, Huo C, Li H, Wang Y, Li Z (2009) Solvent effects on the absorption, circular dichroism and Raman spectroscopy of meso-tetrakis [3-methoxy-4-(N-carbazyl)n-hexyloxyphenyl] porphyrin in water-THF solution. Spectrochim Acta A Mol Biomol Spectrosc 73:581–586
13. Gonçalves PJ, Franzen PL, Correa DS, Almeida LM, Takara M, Ito AS, Zílio SC, Borissevitch IE (2011) Effects of environment on the photophysical characteristics of mesotetrakis methylpyridiniumyl porphyrin (TMPyP). Spectrochim Acta A Mol Biomol Spectrosc 79:1532–1539
14. Jeong H, Huh M, Lee SJ, Koo H, Kwon IC, Jeong SY, Kim K (2011) Photosensitizer-conjugated human serum albumin nanoparticles for effective photodynamic therapy. Theranostics 6:230–239
15. Mataga N, Kubota T (1970) Molecular interactions and electronic spectra. Dekker, New York
16. Kawski A (1966) der Wellenzahl von elecktronenbanden lumineszierenden moleküle. Acta Phys Polon 29:507–518
17. Dabrowski JM, Pereira MM, Arnaut LG, Monteiro CJ, Peixoto AF, Karocki A, Urbańska K, Stochel G (2007) Synthesis, photophysical studies and anticancer activity of a new halogenated water-soluble porphyrin. Photochem Photobiol 83:897–903
18. Nagy PI, Völgyi G, Takács-Novák K (2008) Monte Carlo structure simulations for aqueous 1,4-dioxane solutions. J Phys Chem B 112:2085–2094
19. Allen BD, Benniston AC, Harriman A, Rostron SA, Yu C (2005) The photophysical properties of a julolidine-based molecular rotor. Phys Chem Chem Phys 7:3035–3040
20. Vladimir S, Victor A, Igor V, Tjeerd J, Holten D (2000) Comparative study of the photophysical properties of nonplanar tetraphenylporphyrin and octaethylporphyrin diacids. J Phys Chem B 104:9909–9917
21. Duerr K, Troeppner O, Olah J, Li J, Zahl A, Drewello T, Jux N, Harvey JN, Ivanović-Burmazović I (2012) Solution behavior of iron (III) and iron(II) porphyrins in DMSO and reaction with superoxide. Effect of neighboring positive charge on thermodynamics, kinetics and nature of iron-(su)peroxo product. Dalton Trans 41:546–557
22. Maiti NC, Mazumdar S, Periasamy N (1998) J- and H-aggregates of porphyrin−surfactant complexes: time-resolved fluorescence and other spectroscopic studies. J Phys Chem B 102:1528–1538
23. Melavanki RM, Patil HD, Umapathy S, Kadadevarmath JS (2012) Solvatochromic effect on the photophysical properties of two coumarins. J Fluoresc 22:137–144
24. Weitman H, Schatz S, Gottlieb HE, Kobayashi N, Ehrenberg B (2001) Spectroscopic probing of the acid–base properties and photosensitization of a fluorinated phthalocyanine in organic solutions and liposomes. Photochem Photobiol 73:473–481